Compensation Network Design for MHz-band Wireless Power Transfer in EV Charging Applications

Itsuki MASUDA [1] Sihoon CHOI [1] Mitsuru MASUDA [2]
Jun IMAOKA [2] Masayoshi YAMAMOTO [2]

1) Nagoya University, Electrical Engineering, Nagoya, Aichi, Japan
E-mail: masuda.itsuki.z7@s.mail.nagoya-u.ac.jp
2) Nagoya University, Institute of Materials and Systems for Sustainability, Nagoya, Aichi, Japan

ABSTRACT: This article proposes design guidelines and loss analysis methods for compensation network in capacitive power transfer systems. The design guidelines focus on loss reduction of passive devices and output characteristics (constant current or voltage). By this method, the loss of topology in advance is predicted, and the effect is verifiable. In addition, it allows for a comparison of conventional topologies in a unified manner. The presentation will introduce the proposed topology based on these guidelines.
KEY WORDS: Compensation Network, Capacitive Power Transfer, MHz frequency,

1. INTRODUCTION

Recently, wireless power transfer has entered a transition period from the research phase to the application phase, and its adaptation to electric vehicles and autonomous underwater vehicles is being considered. For example, the spread of this technology to low-power applications such as automatic guided vehicles and electric kickboards is already underway. These applications mainly use inductive power transfer technology in the kHz frequency bands. However, there are also issues such as countermeasures against foreign matter contamination and the cost of litz wires and cores used in couplers. In response to these challenges, capacitive power transfer (CPT) has attracted attention; CPT technology itself was proposed long ago, however, there are few examples of its use in the kHz band due to its low transmission efficiency. On the other hand, recent technological innovations with the advent of GaN and SiC have led to lower loss and higher power in MHz power conversion circuits, and CPT technology is expected to spread.

In order for CPT systems to be widely used, basic research on coupler structure, compensation topology, and EMC measures is needed. In the case of MHz-band CPT systems, the bottleneck for loss and size is the inductor used in the compensation network. Inductors in the MHz-band are broadly classified into the core type and the air-core type. From EMC and size standpoints, core type inductors have advantages. However, magnetic materials in the MHz band have issues with core loss and saturation characteristics, making the selection of core shape and magnetic materials difficult. On the other hand, an air-core inductor has a high radiated electromagnetic field and a large size. Therefore, some approaches have been proposed to minimize the inductor loss and size by devising the topology of the compensation network. The topology using multiple stages of small LC filters reduces overall losses, although the number of elements increases [(1)]. Other than loss reduction, topologies focusing on output characteristics [(2)] and coupler voltage limiting [(3)(4)] have also been proposed. These studies are valid for certain applications. However, it is difficult to select the optimal topology since there is no established indicator with competitive advantages for each topology.

In this study, we propose a method that enables comprehensive evaluation of these compensation networks.

Section 2 provides a configuration of a CPT system for EVs. In addition, we compare proposed compensation network topologies and present some simple guidelines for design. Section 3 clarifies the relation between overall CPT efficiency and compensation network losses. Section 4 discusses the output characteristic analysis method of the compensation network. Section 5 concludes the paper.

2. MHZ BAND CAPACITIVE POWER TRANSFER SYSTEM

2.1. System

Fig. 1 illustrates a simplified configuration of the CPT system. This system comprises three components: the transmitter-side circuit, the coupler, and the receiver-side circuit. The power transmitter-side circuit converts power from the grid into MHz-frequency energy. Therefore, it consists of a Power Factor Correction (PFC) converter, and an MHz-frequency inverter.

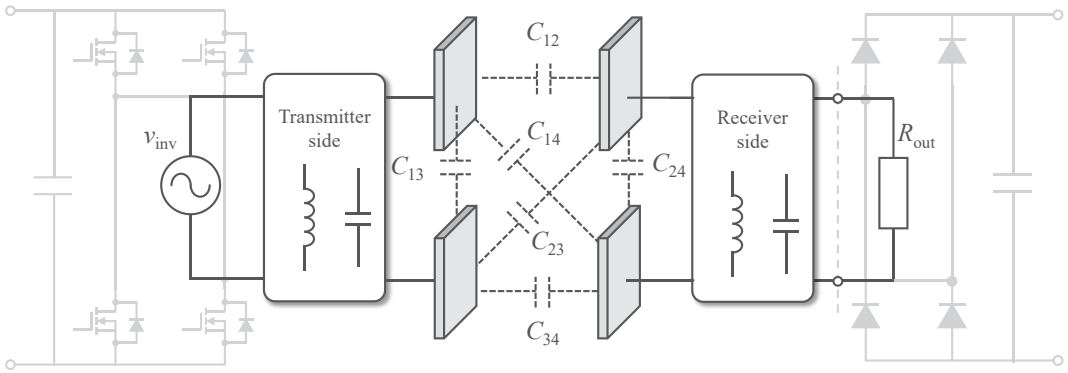

Figure (a)

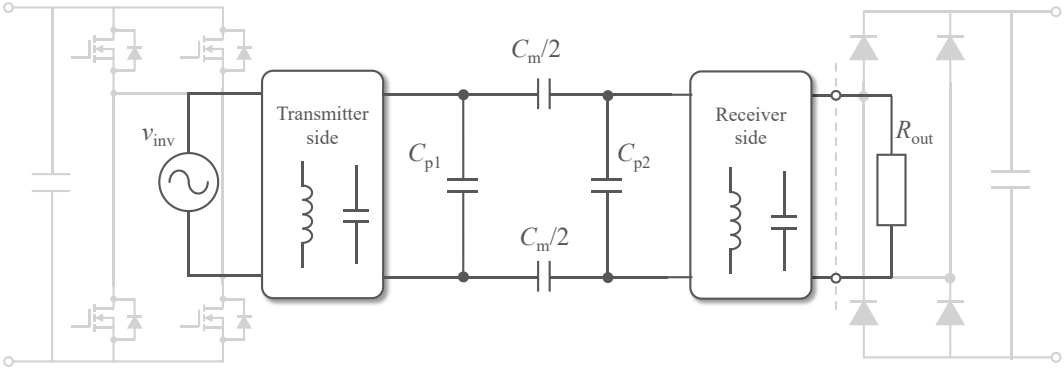

Figure (b)

Fig. 1 Modeling and absorption of parasitic capacitances in a capacitive power transfer system for EV charging. (a) Circuit diagram of all parasitic capacitance (b) Simplified circuit model

Additionally, a compensation network and a low-pass filter (LPF) are connected to the downstream side of the MHz-frequency inverter. In this study, the components upstream of the MHz-frequency inverter (i.e., the AC-DC converter and PFC converter) are treated as an ideal DC power supply. On the other hand, the power receiving circuit is composed of a compensation network, LPF, rectifier circuit, DC-DC converter, and battery.

The combined efficiency of these components determines the overall efficiency of the CPT system. Generally, in MHz-frequency CPT systems, the losses in the MHz-frequency inverter, compensation network, and rectifier circuit are predominant. Specifically, the losses in the compensation network are primarily influenced by the characteristics of the passive components, which tend to increase in high-power systems.

The inverter and rectifier are equivalently represented as v_{inv} and R_{out} using the first harmonic approximation. The coupler is described by six equivalent capacitances, as shown in Fig. 1(a). This represents the bond between each flat plate. By using a combination of series and parallel, and 2-port network theory, the model reduces to a 4-capacitance network, as shown in Fig. 1(b). The equivalent capacitances are given by (1)-(3):

$$C_{p1} = C_{12} + \frac{(C_{13}+C_{14})(C_{23}+C_{24})}{C_{13}+C_{14}+C_{23}+C_{24}} - C_m \quad (1)$$

$$C_{p2} = C_{34} + \frac{(C_{13}+C_{14})(C_{23}+C_{24})}{C_{13}+C_{14}+C_{23}+C_{24}} - C_m \quad (2)$$

$$C_m = \frac{C_{24}C_{13} - C_{14}C_{23}}{C_{13}+C_{14}+C_{23}+C_{24}} \quad (3)$$

2.2. Topology and design guidelines

In CPT systems, the compensation network topology is particularly important in terms of efficiency and size. Table 1 shows the topologies proposed for the CPT system and their characteristics [5][6]. These topologies are used for different applications and purposes. There are fewer simple topologies, such as series-serial (S-S) topologies, compared to inductive power transfer systems. Many topologies incorporating three or more passive components have been proposed, based on several considerations outlined below:

- Maximum efficiency - coupler and compensation network
- Maximum output power - Breakdown voltage at the coupler
- Output characteristics - Constant current or Constant voltage
- Harmonic characteristics – LPF characteristics
- Size and cost – Inductors are especially important

3. RELATION BETWEEN EFFICIENCY AND COMPENSATION NETWORK

3.1. Maximum Efficiency

This section discusses the relation between coupler efficiency and compensation network. The maximum coupler efficiency $\eta_{\max}$ is expressed using the impedance matrix $\mathbf{Z}$ of the coupler as follows (4)-(5):

$$\eta_{\max} = \frac{\sqrt{\Sigma} - \sqrt{\Delta}}{\sqrt{\Sigma} + \sqrt{\Delta}} \tag{4}$$

$$\boldsymbol{Z} = \begin{bmatrix} Z_{11} & Z_{12} \\ Z_{21} & Z_{22} \end{bmatrix} = \begin{bmatrix} R_{11} + jX_{11} & R_{12} + jX_{12} \\ R_{21} + jX_{21} & R_{22} + jX_{22} \end{bmatrix} \tag{5}$$

where Σ and Δ are defined by (6):

$$\begin{cases} \Sigma = R_{11}R_{22} + X_{12}X_{21} \\ \Delta = \mathrm{R}_{11}R_{22} - R_{12}R_{21} \end{cases} \tag{6}$$

The reciprocity is assumed to be valid, and isolators and circulators are not covered. The receiving side impedance Z_{opt} needs to be set as follows (7):

$$Z_{\mathrm{opt}} = R_{\mathrm{opt}} + jX_{\mathrm{opt}} = \frac{\sqrt{\Sigma\Delta}}{R_{11}} + j\left(\frac{R_{12}X_{21}}{R_{11}} - X_{22}\right) \tag{7}$$

Therefore, the compensation network on the receiving side just needs to convert the load impedance to the optimum impedance. Under this optimum load impedance condition, the input impedance of the coupler Z_{in} becomes is derived as follows (8):

$$Z_{\mathrm{in}} = R_{\mathrm{in}} + jX_{\mathrm{in}} = \frac{\sqrt{\Sigma\Delta}}{R_{22}} + j\left(X_{11} - \frac{R_{12}X_{21}}{R_{22}}\right) \tag{8}$$

The compensation network on the transmitter side is designed to compensate for the imaginary part of the input impedance X_{in}. In general, Class-D or Class-E inverters are used on the input side, so the input impedance needs to be inductive for zero volt switching operation. In addition, the real part of the input impedance R_{in} is also important for optimal inverter operation.

3.2. Loss Analysis of Passive Devices

The compensation network consists only of an inductor and a capacitor in series or parallel as shown in Fig. 2. Z_{N} is the output impedance of passive devices, and Y_{N} is the output admittance. Although the use of a transformer is also considered, equivalently, it is expressed only by an inductor. The combination of these

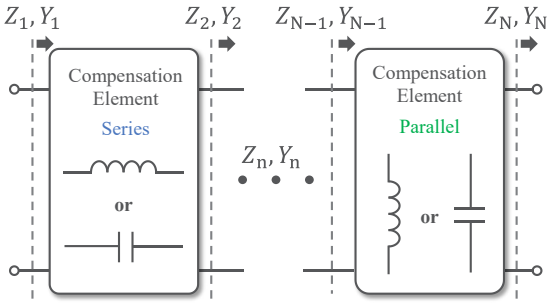

Fig. 2 Basic compensation network configuration

devices performs impedance transformation, although attention should be paid to the differences in device stresses and losses due to topology and number of stages.

There is the relation between the efficiency of the compensation network and the distance on the Smith chart (Poincaré length) as follows (9) [7]:

$$-\log_e \eta = \frac{1}{\sqrt{1+Q^2}}\Lambda \tag{9}$$

where η is the compensation efficiency, Q is the quality factor of the component and Λ is the hyperbolic length of the path on Smith chart, which is defined (10).

$$\Lambda = \int_Z \frac{1}{\mathrm{Re}(Z)}|dZ| = \int_Y \frac{1}{\mathrm{Re}(Y)}|dY| \tag{10}$$

In the compensation network with inductor or capacitor, there is no change in the resistance component in series connection and the conductance component in parallel connection. Therefore, (10) becomes (11)-(12):

$$\Lambda_{\mathrm{series}} = \int_{X_1}^{X_2} \frac{1}{\mathrm{Re}(Z)}|dX| \tag{11}$$

$$\Lambda_{\mathrm{parallel}} = \int_{B_1}^{B_2} \frac{1}{\mathrm{Re}(Y)}|dB| \tag{12}$$

where $\Lambda_{\mathrm{series}}$ is the hyperbolic length in series connection and $\Lambda_{\mathrm{parallel}}$ is the hyperbolic length in parallel connection. In the case of a multi-stage compensation network, the relation between the hyperbolic length and the overall efficiency of the compensation network is expressed as follows (13):

Table.1 Compensation network topologies for CPT system

Reference	2	3	4	5
Frequency	800kHz	1MHz	400kHz	1MHz
Output power	2kW	1.87kW	1.94kW	2.4kW
Efficiency	90.29%	85.87%	95.50%	90.80%
Compensation Topology	LC-CLC	LCL-LCL	S-S	LCLC-LCLC
Output Characteristics	-	Constant current	Constant current	-
Puerpose	・Management of coupler voltage phase ・ Minimum Plate Voltage Stresses	・Minimum Plate Voltage Stresses ・Low-pass filter for inverter and rectifier	・Unity power factor at input and output ・Simple configuration with a small number of elements	・Unity power factor at input and output ・Low-pass filter for inverter and rectifier

$$-\log_e \eta = \sum_{n=1}^{N} \frac{1}{\sqrt{1+Q_n^2}} \Lambda_n \quad (13)$$

where n is the number of stages in the compensation network and Q_n is the Q factor of the passive component itself. In many cases in the MHz frequency band, capacitors have lower losses than inductors, and inductors account for most of the losses (i.e., $Q_C >> Q_L$). Therefore, it is important to use a topology that reduces inductor losses to achieve high efficiency.

3.3. Output Characteristics

This section describes the voltage-current characteristics when the output resistance is varied. In actual applications, efficiency and power characteristics are important, although output voltage and current characteristics are also important characteristics. This section describes how to determine the output characteristics of these topologies using the impedance matrix of the compensation network.

Fig. 3 shows the coupler and impedance matrix of the compensation network. Z_{aa} to Z_{dd} represent the impedance matrices of the compensation network. Since the coupler has an immittance characteristic, the power supply characteristics (voltage source or current source) change between the input and output sides. Therefore, when the compensation network has either an immittance or transformer characteristic, the constant output characteristic is obtained with respect to load variations. This article discusses the compensation circuit on the transmitter side and shows how to determine the output characteristics.

Fig. 4 (a) shows the equivalent circuit of the transmitter side compensation network, and the inverter transformed by Thevenin's theorem. The equivalent voltage source is determined independent of the load side. The equivalent series impedance Z_{equ} is expressed by (14):

$$Z_{\mathrm{equ}} = jX_{\mathrm{equ}} = X_{\mathrm{bb}} - \frac{X_{\mathrm{ab}}^2}{X_{\mathrm{aa}}} \quad (14)$$

where the compensation network is lossless. In the case that X_{equ}=0, it is a constant voltage source characteristic with respect to the load impedance from the Thevenin's theorem. The same phenomenon is observed on either the transmitter or receiver side due to reciprocity. The conditions under which the constant voltage source characteristic can be obtained are as follows (15):

$$X_{\mathrm{aa}} X_{\mathrm{bb}} = X_{\mathrm{ab}}^2 \quad (15)$$

According to (15), the constant voltage characteristic can be determined by determining the impedance matrix of the compensation network. In addition, when the input side is shorted in the actual measurement, the output impedance is (16)

$$Z_{\mathrm{out(0)}} = X_{\mathrm{bb}} - \frac{X_{\mathrm{ab}}^2}{X_{\mathrm{aa}}} \quad (16)$$

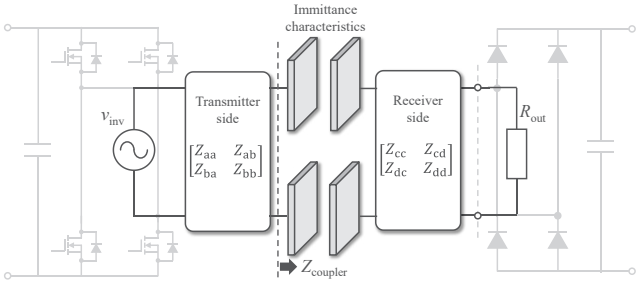

Fig. 3 Coupler and compensation network

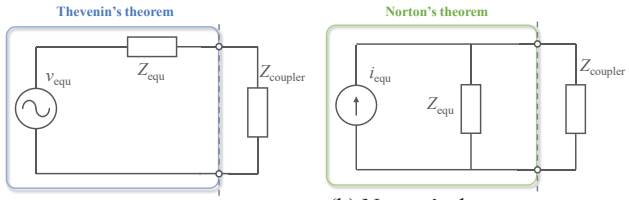

(a) Thevenin's theorem (b) Norton's theorem

Fig. 4 Equivalent circuit of compensation network

where it is clear that a more ideal constant voltage characteristic can be obtained with (13) close to 0.

Fig. 4 (b) shows the equivalent circuit of the transmitter side compensation network, and the inverter transformed by Norton's theorem. As in Thevenin's theorem, the equivalent current source is determined independent of the load side, and the equivalent parallel admittance Y_{equ} is expressed by (17):

$$Y_{\mathrm{equ}} = jB_{\mathrm{equ}} = B_{\mathrm{bb}} - \frac{B_{\mathrm{ab}}^2}{B_{\mathrm{aa}}} \quad (17)$$

where B_{aa} to B_{bb} are susceptance matrices of compensation networks, and the compensation network is lossless. The conditions under which the constant current source characteristic can be obtained are as follows (18):

$$B_{\mathrm{aa}} B_{\mathrm{bb}} = B_{\mathrm{ab}}^2 \quad (18)$$

According to (15), the constant current characteristic can be determined by determining the admittance matrix of the compensation network. In addition, when the input side is open in the actual measurement, the output admittance is (19)

$$Y_{\mathrm{out}(\infty)} = B_{\mathrm{bb}} - \frac{B_{\mathrm{ab}}^2}{B_{\mathrm{aa}}} \quad (19)$$

where a more ideal constant voltage characteristic can be obtained with (16) close to 0.

4. PROPOSED COMPENSATION NETWORK

4.1. Circuit Configuration

Fig. 5 (a) illustrates a configuration with an L-type network on the transmitter side and an inverted L-type network on the receiver side (T_1-R_1). The advantages of this circuit are its design simplicity

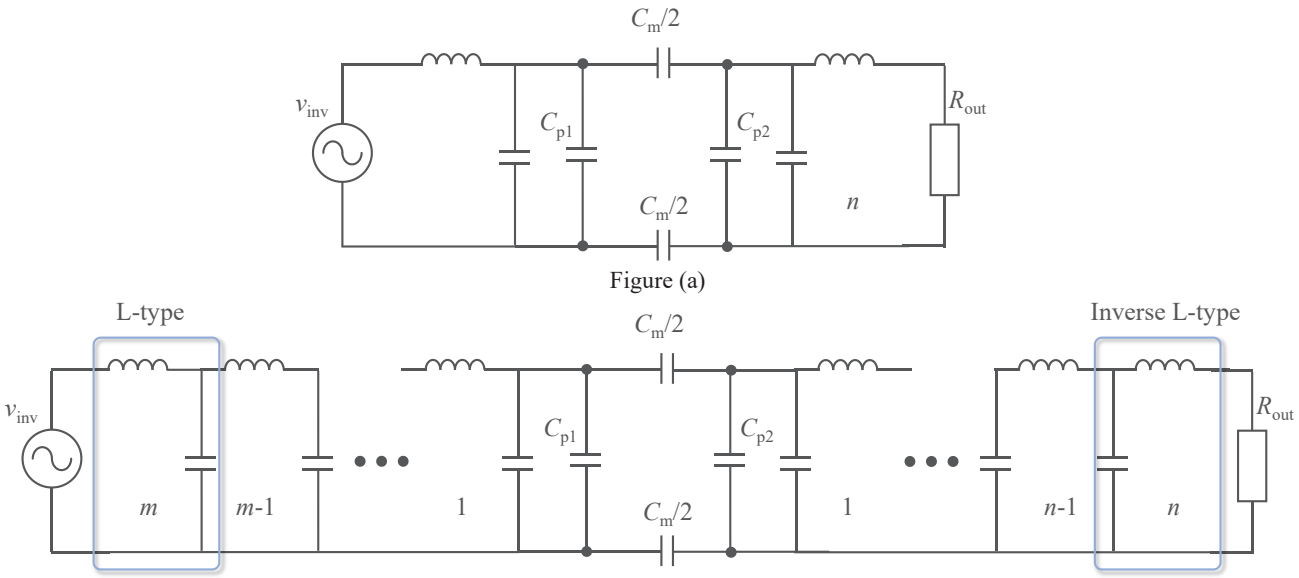

Figure (a)

Figure (b)

Fig. 5 Circuit configuration of conventional and proposed (a) Transmitter side: an L-type, Receiver side: an inverted L-type (T_1-R_1) (b) Transmitter side: m L-type, Receiver side: n inverted L-type (T_m-R_n)

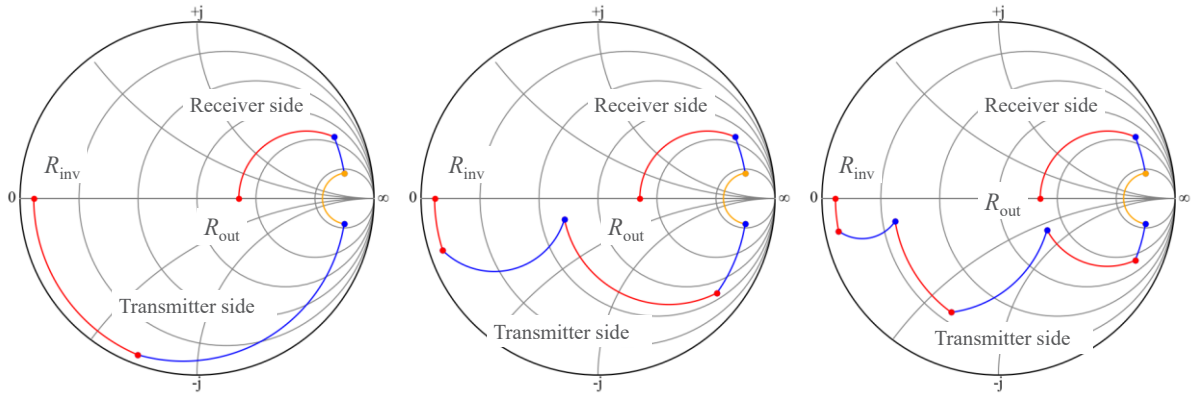

Figure (a) Figure (b) Figure (c)

Fig. 6 Impedance transformation trajectories of conventional and proposed compensation networks on the smith chart. The yellow line represents the coupler's coupling capacitor C_m. (a) Transmitter side: an L-type, Receiver side: an inverted L-type (T_1-R_1) (b) Transmitter side: 2 L-type, Receiver side: an inverted L-type (T_2-R_1) (c) Transmitter side: 3 L-type, Receiver side: an inverted L-type (T_3-R_1)

and the reduced number of components. However, the input and output impedance adjustments must be made using C_{t1} and C_{r1}, which are connected to the coupler, resulting in limited design flexibility. Fig. 5 (b) illustrates a configuration with m L-type networks on the transmitter side and n inverted L-type networks on the receiver side (T_m-R_n). This topology allows the number of stages on the transmitter and receiver sides to be adjusted arbitrarily based on the input and output impedance, providing greater design flexibility.

The inverter connected to the transmitter side requires a low-impedance output to achieve zero voltage switching operation and high efficiency [][]. The impedance is matched with the high-impedance coupler side. This generally requires a large impedance transformation ratio. On the other hand, the receiver side can operate while maintaining a high-impedance, since a DC-DC converter is connected after the rectifier. A large impedance transformation ratio is not required for the matching circuit on the receiver side. In this study, the compensation networks and designed assuming an input impedance of 20Ω and an output impedance of 810Ω. The system size is set with reference to SAE J2954, the standard for a inductive power transfer, with a transmission distance of 160mm and coupler size of 340mm × 340mm.

4.2. Comparison of Conventional and Proposed Topologies

Fig. 6 shows the Smith chart trajectories for different numbers of stages on the transmitter side. Table.2 presents the

corresponding Poincaré length and component values. The yellow line represents the coupler's coupling capacitor C_m. The upper side of the Smith chart corresponds to the receiver compensation network, while the lower side corresponds to the transmitter compensation network. The proposed multi-stage L-type topology is designed for efficiency optimization, based on (13). The efficiency optimized for the Poincaré length is as follows (20):

$$-\log_e \eta_{\max} = \frac{2}{Q_L}\left(mQ_{\max} - (m-1)\,Q_{\max}^{-1}\right) \tag{20}$$

where the trajectory of the multi-stage L-type network must pass within the conditions defined by $Q_{\min}$ and $Q_{\max}$.

$$Q_{\max}^{2(m-1)} + Q_{\max}^{2m} = \frac{|X_{C_m}|}{R_{\text{inv}}} \tag{21}$$

$$Q_{\min} = Q_{\max}^{-1} \tag{22}$$

Based on (21), the Poincaré length ideally decreases as the number of stages increases. This is also shown in Fig. 6.

Fig. 7 illustrates the inductor Q factor and the efficiency/loss characteristics of each topology. These simulations were conducted assuming an output power of 1kW. These results indicate that efficiency increases as the number of stages increases. In the conventional 1-stage and the proposed 2-stage configurations, a 5-point improvement is observed for a Q factor below 200. Even for a Q factor above 200, an improvement of approximately 3 points is demonstrated. Fig. 7 (b) shows the total loss of the compensation network for Q=100. These results indicate that the improvement effect diminishes as the number of stages increases. The most significant improvement is observed when using a 2-stage configuration.

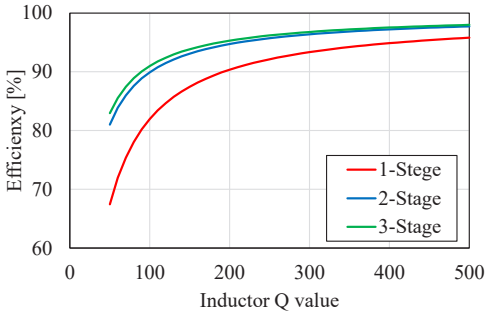

Figure (a)

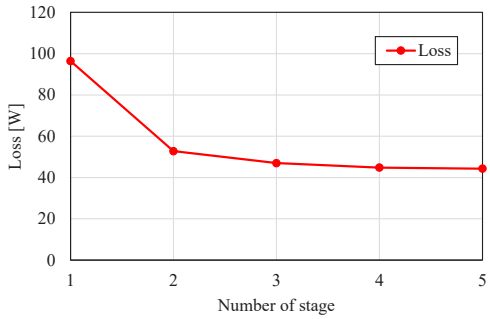

Figure (b)

Fig. 7 Inductor Q factor and efficiency/loss characteristics of each topology (a) Relation inductor Q factor and Efficiency (b) Total loss of the compensation network for Q=100

5. CONCLUSION

Design guidelines for compensation network are summarized and their relation to efficiency and output characteristics. Compensation networks have been discussed for each application and each has its own advantages. This article summarizes these characteristics and provides guidelines for their evaluation in a unified manner. In addition, we have summarized methods for evaluating output characteristics. In addition, we have summarized methods for evaluating output characteristics. These guidelines are applicable to compensation circuits for CPT systems as well as IPT systems and MHz inverters. The presentation will introduce the proposed topology based on these guidelines. ssWe will also discuss the differences from conventional topologies.

REFERENCES

(1) S. Sinha, A. Kumar, B. Regensburger and K. K. Afridi, "Design of High-Efficiency Matching Networks for Capacitive Wireless Power Transfer Systems," in *IEEE Journal of Emerging and Selected Topics in Power Electronics*, vol. 10, no. 1, pp. 104-127, Feb. 2022.

(2) Y. Liu, X. L. Li, C. K. Tse and C. Zhu, "A Comparative Study of Compensation Topologies for Capacitive Power Transfer based on Sensitivity Analysis," *ICPE 2023 - ECCE Asia*, Jeju Island, Korea, Republic of, 2023.

(3) H. Zhang, F. Lu, H. Hofmann, W. Liu and C. C. Mi, "A Four-Plate Compact Capacitive Coupler Design and LCL-Compensated Topology for Capacitive Power Transfer in Electric Vehicle Charging Application," in *IEEE Transactions on Power Electronics*, vol. 31, no. 12, pp. 8541-8551, Dec. 2016

(4) B. Luo, A. P. Hu, H. Munir, Q. Zhu, R. Mai and Z. He, "Compensation Network Design of CPT Systems for Achieving Maximum Power Transfer Under Coupling Voltage Constraints," in *IEEE Journal of Emerging and Selected Topics in Power Electronics*, vol. 10, no. 1, pp. 138-148, Feb. 2022.

(5) T. Imura, K. Suzuki, K. Hata, and Y. Hori, “Comparison of Four Resonant Topologies Based on Unified Design Procedure for Capacitive Power Transfer,” in *IEEJ Journal of Industry Application*, vol. 10, No. 3, pp. 339-347, 2021.

(6) T. Chen, C. Cheng, X. Zhang, G. Li, Y. Guo and C. C. Mi, "A Double-Sided LCL-Compensated Network for the

Strongly Coupled CPT System With Minimum Plate Voltage Stresses," in *IEEE Journal of Emerging and Selected Topics in Power Electronics*, vol. 12, no. 4, pp. 4275-4287, Aug. 2024.

(7) K. Yamada and T. Ohira, "Graphical Representation of the Power Transfer Efficiency of Lumped-Element Circuits Based on Hyperbolic Geometry," in *IEEE Transactions on Circuits and Systems II: Express Briefs*, vol. 64, no. 5, pp. 485-489, May 2017.